Journal of Luminescence 169 (2016) 400–405

Contents lists available at ScienceDirect

Journal of Luminescence

journal homepage: www.elsevier.com/locate/jlumin

Mid infrared lasers for remote sensing applications

Brian M. Walsh [a,*], Hyung R. Lee [b], Norman P. Barnes [c]

[a] NASA Langley Research Center, Hampton, VA 23681, USA
[b] National Institute of Aerospace, Hampton, VA 23666, USA
[c] Science Systems and Applications, Inc., Hampton, VA 23666, USA

ARTICLE INFO

Article history:
Received 8 October 2014
Received in revised form
6 March 2015
Accepted 8 March 2015
Available online 16 March 2015

Keywords:
Lanthanide-doped materials
Low phonon materials
Mid-infrared lasers
Atmospheric remote sensing

ABSTRACT

To accurately measure the concentrations of atmospheric gasses, especially the gasses with low concentrations, strong absorption features must be accessed. Each molecular species or constituent has characteristic mid-infrared absorption features by which either column content or range resolved concentrations can be measured. Because of these characteristic absorption features the mid infrared spectral region is known as the fingerprint region. However, as noted by the Decadal Survey, mid-infrared solid-state lasers needed for DIAL systems are not available. The primary reason is associated with short upper laser level lifetimes of mid infrared transitions. Energy gaps between the energy levels that produce mid-infrared laser transitions are small, promoting rapid nonradiative quenching. Nonradiative quenching is a multiphonon process, the more phonons needed, the smaller the effect. More low energy phonons are required to span an energy gap than high energy phonons. Thus, low energy phonon materials have less nonradiative quenching compared to high energy phonon materials. Common laser materials, such as oxides like YAG, are high phonon energy materials, while fluorides, chlorides and bromides are low phonon materials. Work at NASA Langley is focused on a systematic search for novel lanthanide-doped mid-infrared solid-state lasers using both quantum mechanical models (theoretical) and spectroscopy (experimental) techniques. Only the best candidates are chosen for laser studies. The capabilities of modeling materials, experimental challenges, material properties, spectroscopy, and prospects for lanthanide-doped mid-infrared solid-state laser devices will be presented.

Published by Elsevier B.V.

1. Introduction

Mid infrared (MIR) differential absorption lidar (DIAL) systems can provide vital data needed by atmospheric scientists to understand atmospheric chemistry. The Decadal Survey [1] recommended missions to measure atmospheric constituents including CO_2, CH_4, CO, O_3, NO_2, SO_2, and CH_2O. All of the atmospheric constituents noted above have unique and useful characteristic absorption features in the mid infrared, as shown in Table 1 where significant absorption of a constituent exists. In addition, the characteristic absorption can be found in spectral windows where the atmospheric transmission is relatively good, as shown in Fig. 1. Thus, when developed, mid infrared lasers will be able to measure all of the atmospheric constituents requested by the Decadal Survey.

While there are a variety of choices for MIR laser, each has various tradeoffs and the application to specific measurements must be considered as well [2]. Semiconductor Lasers (Lead-Salt, Quantum Cascade and Antimonide III–V) are possibilities, but may require cryogenic cooling and have highly divergent, astigmatic beams. Solid State lasers, such as Cr^{2+} II–VI lasers, are generally low gain materials, resulting in low power/energy. Parametric frequency conversion, such as optical parametric oscillator (OPO) and difference frequency generation (DFG) suffer from a variety of drawbacks including phase matching, design complexity, alignment sensitivity, and laser induced damage (LID). Laser pumped Ln^{3+} (lanthanide) lasers offer a main advantage of pump energy storage, as well as high power or energy output in a narrow spectral bandwidth and diffraction limited beam, which are some specific reasons to select them over other technologies for some remote sensing applications. A wide variety of pulse widths and pulse repetition frequencies (from cw to 1 GHz) can also be achieved. Ln^{3+} lasers, in particular, offer broad tunability, efficient operation via direct diode pumping, a variety of pulse lengths and repetition frequencies in pulsed mode, and good beam quality. Operating in the MIR the Ln^{3+} lasers can access atmospheric transmission windows in the $\sim$3–5 μm and 7–10 μm regions. The $\sim$5–7 μm region is not so useful due to the presence of high water vapor absorption. Some explanation should be made regarding the meaning of mid infrared, which can be rather ambiguous. Generally it is used to encompass the 3–8 μm region, which comprises the mid wavelength infrared (MWIR) and long

* Corresponding author. Tel.: +1 757 864 7112; fax: +1 757 864 8828.
E-mail address: brian.m.walsh@nasa.gov (B.M. Walsh).

http://dx.doi.org/10.1016/j.jlumin.2015.03.004
0022-2313/Published by Elsevier B.V.

Table 1
Atmospheric constituents identified by characteristic absorption features.

Molecular species	Wavelength windows (μm)		
	3.00–4.00	4.50–5.00	7.0–10.0
CH_4	3.15–3.57		< 7.5–8.3
CO		4.50–4.87	
O_3		4.70–4.79	9.37–9.90
NO_2	3.40–3.85	4.45–4.70	7.50–8.10
SO_2			7.13–7.75
CH_2O	3.20–3.40		

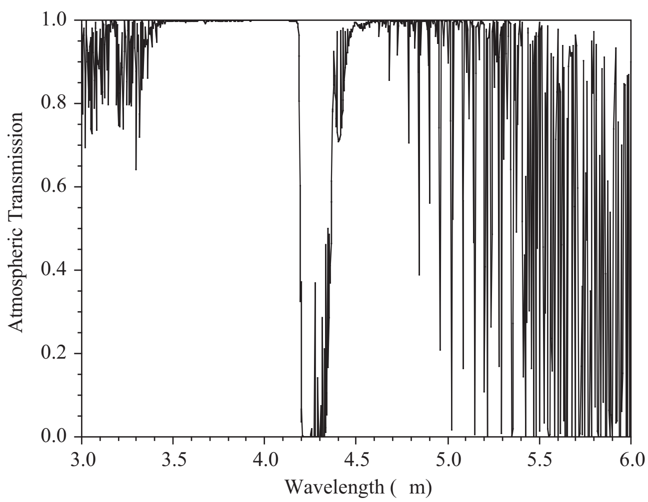

Fig. 1. Atmospheric transmission from 3 to 6 μm.

Table 2
Infrared spectral ranges.

Division name	Abbreviation	Wavelength (μm)
Near infrared	NIR	0.75–1.4
Short wavelength infrared	SWIR	1.4–3
Mid wavelength infrared	MWIR	3–8
Long-wavelength infrared	LWIR	8–15
Far infrared	FIR	15–1000

wavelength infrared (LWIR) divisions, and is sometimes used at shorter wavelengths such as 2 μm. In Table 2, the various divisions of the infrared spectral ranges are given for reference.

Most lanthanide or transition metal doped solid-state materials can produce laser wavelengths in the ultraviolet (UV), visible (VIS), or short wavelength infrared (SWIR). However, it becomes increasingly difficult to generate wavelengths in the mid-wavelength infrared (MWIR) and beyond. We will use the term MIR to refer to the MWIR wavelength ranges as defined in Table 2. The great challenge in solid-state lasers for MIR operation is finding materials that offer low phonon energies. Solid-state lasers that have wavelengths longer than about 2.5 µm are usually quenched by nonradiative processes. These nonradiative processes are caused by high energy crystal lattice vibrations called phonons. When the energy gap between 2 energetically adjacent manifolds is less than 5 times the maximum phonon energy, the nonradiative transitions tend to quench the upper manifold. Hence, to develop an efficient MIR laser with a wavelength longer than ~2.5 µm requires a low phonon energy host material.

In general oxides have the largest phonon energies, followed by fluorides, chlorides, bromides and iodides. However, having a low phonon energy is not the only criterion in choosing a material. The

Table 3
Crystal phonon energies and optical transparency range.

Formula	Material name	Phonon energies (cm^{-1})	Transparency (μm)
YVO_4	Yttrium vanadate	880–980	0.35–4.8
$Y_3Al_5O_{12}$	Yttrium aluminum garnet	700–850	0.21–5.2
$YAlO_3$	Yttrium aluminum oxide	550–600	0.20–7.0
Y_2O_3	Yttrium oxide	400–600	0.29–7.1
$YLiF_4$	Yttrium lithium fluoride	400–560	0.12–8.0
$CaGa_2S_4$	Calcium gallium sulfide	350–400	0.34–12
BaY_2F_8	Barium yttrium fluoride	350–415	0.20–9.5
KYF_4	Potassium yttrium fluoride	350–400	0.15–9.0
LaF_3	Lanthanum fluoride	300–350	0.20–10
CaF_2	Calcium fluoride	280–330	0.20–10
$LaCl_3$	Lanthanum chloride	240–260	0.30–25
KPb_2Cl_5	Potassium lead chloride	200	0.30–16
$LaBr_3$	Lanthanum bromide	175	0.30–20
$CsCdBr_3$	Cesium cadmium bromide	150–160	0.40–25
KPb_2Br_5	Potassium lead bromide	140	0.40–25

optical transparency is important as well. Table 3 lists the phonon energy and transparency range for a variety of crystal laser materials.

Clearly the oxides do not make good choices either in phonon energy or optical transparency. This leaves choices of fluorides, chlorides and bromides for materials with appealing phonon energies. Another issue to consider is the hygroscopic nature of the material, or the ability to readily absorb moisture. Fluorides tend to be weakly hygroscopic, while chlorides and bromides show varying degrees depending on the composition. For example, $LaCl_3$ and $LaBr_3$ are highly hygroscopic, while KPb_2Cl_5 and KPb_2Br_5 are only mildly hygroscopic. Prudent material choices, based on Table 3 as well as hygroscopic issues are BaY_2F_8, KYF_4, LaF_3, KPb_2Cl_5, $CsCdBr_3$ and KPb_2Br_5 materials.

Keeping the importance of the host material in mind we will proceed in a systematic way, discussing the lanthanide ions and manifold-to-manifold pairs which offer MIR transitions, followed by material selection and laser prospects. Some emission spectroscopy results for praseodymium (Pr) in the 3–6 μm region is also presented.

2. Materials and methods

Selection of the laser material and the specific lanthanide series atom can be made essentially independently. The choice of laser material exerts only a small influence on the 4f electrons because of the shielding of the 5s and 5p electrons. Consequently, the choice of laser material affects the energy levels and manifolds only slightly. Thus, a promising pair of manifolds in a particular laser material will have essentially the same pair of manifolds in another material. If the particular wavelength is not critical, the largest effect in the choice of laser material is the maximum phonon energy.

2.1. Laser ions and manifold pairs

Lanthanide series atoms were reviewed to identify potential manifold pairs suitable for mid infrared lasers. The qualities sought include

1. An energy gap between a pair of manifolds that generates the desired wavelength.
2. As large of an energy gap as practical between the upper and lower laser manifolds.

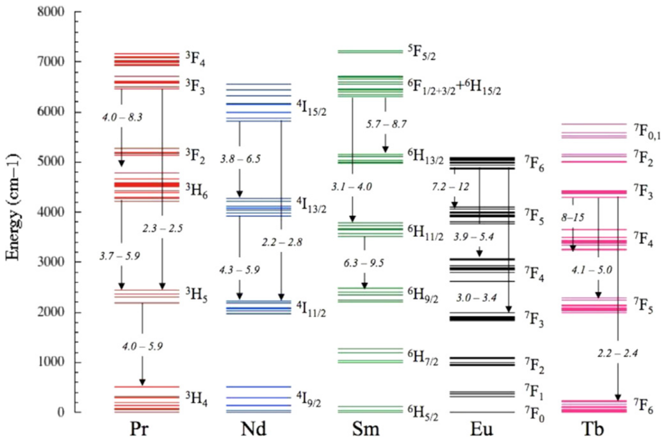

Fig. 2. Mid infrared transitions in Pr, Nd, Sm, Eu and Tb ions.

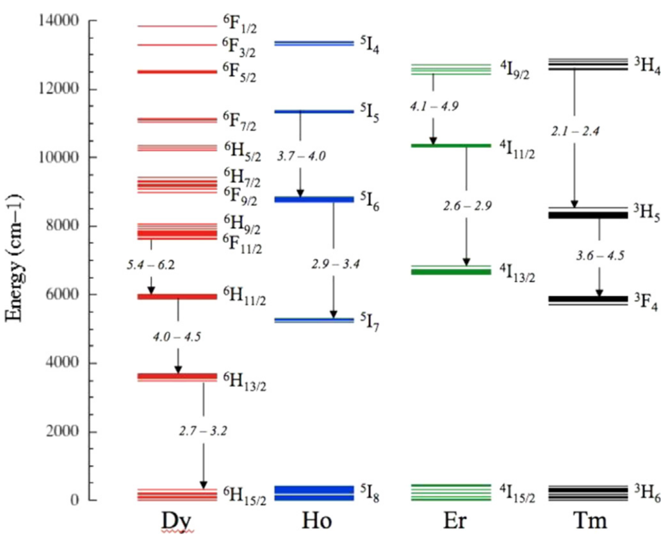

Fig. 3. Mid infrared transitions in Dy, Ho, Er and Tm ions.

3. A low thermal population residing in the lower laser level.
4. A small energy gap between the lower laser manifold and the next lower manifold.
5. An absorption feature that is compatible with laser pumping.

An analysis of the lanthanide series atoms yields at least a number of manifold pairs favorable for mid infrared lasers. These possibilities are discussed individually and in some detail below. Energy level diagrams for various possibilities are included in Figs. 2 and 3 for facile reference. For initial study, the energy levels for LaF_3 were utilized primarily because of availability. Manifolds and energy levels for other materials with low phonon energy are expected to be only slightly different. The total possibilities are too extensive for all lanthanide atoms in all materials to be analyzed, but by using published energy levels of LaF_3, a wide range of manifold pairs of lanthanide series atoms can be inferred. The results are in Table 4. In this table upper gap means the energy gap between the upper laser level manifold and the next highest manifold, while lower gap means the energy gap between the lower laser manifold and the next highest manifold. Both are important to consider.

A few definitions are in order, and the various types of solid-state lasers are shown in Fig. 4 for reference. When an atom in a 4 level laser transitions from the upper laser manifold to the lower laser manifold the population inversion decreases by 1 quantum. There is 1 less atom in the upper laser manifold and the added population in the lower laser manifold rapidly decays. Nd:YAG operating at 1.06 μm is a good example of a 4 level laser. If the lower laser level does not decay rapidly, it is called a terminated 4 level laser. Dy:YLF operating at 4.3 μm is an example of a terminated 4-level laser. When an atom in a 3-level laser transitions from the upper laser manifold to the lower laser manifold, there is 1 less atom in the upper laser manifold and 1 more atom in the lower laser manifold. This decreases the population inversion by 2. The ruby laser ($Cr:Al_2O_3$) operating at ~0.7 μm is an example of a 3-level laser. Lasers that are between 3 and 4-level lasers are characterized by a factor describing how the population inversion changes when 1 atom transitions. If this factor is less than 1.5, it is quasi 4-level laser. Quasi 4-level lasers have a high threshold because the lower laser level thermal population must be overcome to achieve a positive gain. Ho:YAG operating at 2.1 μm is a good example of a quasi 4-level laser.

2.1.1. *Praseodymium*

A Pr laser can be pumped from the $^3H_4$ manifold to the $^3F_3$ manifold with laser diodes around 1.55 μm or an Er fiber laser. From the $^3F_3$ manifold, laser action may be possible to the $^3F_2$ manifold with wavelengths in the 6–8 μm band. Because of the small energy gap the maximum phonon energy of the laser material should be 200 cm^{-1} or less. If this is not available, the pump laser can be operated Q-switched. The lower laser manifold will quickly relax to the $^3H_6$ manifold. Conversely, the $^3H_6$ manifold may by pumped with a Tm:fiber laser or a diode laser around 1.9 μm. Laser action can then proceed to the $^3H_5$ manifold that produces wavelengths in the 4–6 μm band. This will tend to be a terminated 4 level laser. The possibility also exists for laser action from the $^3H_5$ to $^3H_4$ manifold, also producing wavelengths in the 4–6 μm band, but in this case it will be a quasi 4-level laser. Bowman has reported laser emission at 5 and 7 μm in $Pr:LaCl_3$ [3].

2.1.2. *Neodymium*

A Nd mid infrared laser can be pumped directly with laser diodes or with an Er laser, either an Er:fiber laser or a bulk Er laser. There are 2 possible useful transitions, the $^4I_{15/2}$ to $^4I_{13/2}$ transition and the $^4I_{13/2}$ to $^4I_{11/2}$ transition. Both of these transitions would generate wavelengths in the 4–6 μm region but neither is considered to be a quasi 4-level laser. There is a possibility for cascade lasing as the lower manifold of the first transition is the upper laser level for the second transition. It does not appear that Nd will be able to generate an output above ~7 μm region. Because the energy gaps between the manifolds are nearly equal, there is a compromise between energy storage and terminated laser operation. This compromise can be addressed by the choice of the laser material. If needed, energy can be stored in a bulk Er pump laser.

2.1.3. *Samarium*

A Sm laser can be pumped from the $^6H_{5/2}$ manifold to the $^6H_{15/2}$ manifold with an Er laser. The Er laser could be an Er:fiber laser, a bulk Er:YAG laser or laser diodes. The $^6H_{15/2}$ manifold has potential as a storage manifold, depending on the choice of material. By Q-switching the $^6F_{15/2}$ manifold to the $^6H_{11/2}$ manifold transition, a population inversion between the $^6H_{11/2}$ manifold and the $^6H_{9/2}$ manifold or the $^6H_{11/2}$ manifold and the $^6H_{7/2}$ manifold can be established. This can happen despite the relatively small energy gaps to the next lower manifold. An output in the 3–4 μm region and in the 6–8 μm region may be possible. Which of these transitions will achieve threshold first depends on cross sections and branching ratios. In either case, the small energy gap to the next lower manifold indicates a rapid depopulation of the lower laser manifold and therefore 4 level laser operation. It is possible that both transitions may operate efficiently. The $^6H_{13/2}$ to $^6H_{11/2}$ transition is also a possibility, pumped by Ho:YAG, Tm:fiber or diode lasers.

Table 4
Potential mid infrared laser systems.

Crystal	Pump laser	Storage level	Upper level	Lower level	Wavelength range (μm)	Upper gap (cm^{-1})	Lower gap (cm^{-1})
$Pr:LaF_3$	Ho:YAG	$^3F_3$	$^3F_3$	$^3F_2+^3H_6$	4.0–8.3	1201	1695
$Pr:LaF_3$	Ho:YAG	$^3H_6$	$^3H_6$	$^3H_5$	3.7–5.9	1695	1690
$Pr:LaF_3$	Ho:YAG	$^3H_6$	$^3H_5$	$^3H_4$	4.0–5.9	1690	0
$Nd:LaF_3$	Er:YAG	$^4I_{15/2}$	$^4I_{15/2}$	$^4I_{13/2}$	3.8–6.5	1535	1694
$Nd:LaF_3$	Cr:ZnSe	$^4I_{13/2}$	$^4I_{13/2}$	$^4I_{11/2}$	4.3–5.9	1694	1480
$Sm:LaF_3$	Er:YAG	$^6H_{15/2}$	$^6H_{15/2}$	$^6H_{13/2}$	5.7–8.7	1149	1185
$Sm:LaF_3$	Er:YAG	$^6H_{15/2}$	$^6H_{15/2}$	$^6H_{11/2}$	3.1–4.0	1185	1054
$Sm:LaF_3$	Ho:YAG	$^6H_{13/2}$	$^6H_{13/2}$	$^6H_{11/2}$	6.1–8.4	1185	1054
$Sm:LaF_3$	Er:YAG	$^6H_{11/2}$	$^6H_{11/2}$	$^6H_{9/2}$	6.3–9.5	1054	929
$Eu:LaF_3$	Tm:gls	$^7F_6$	$^7F_6$	$^7F_5$	7.2–12.0	813	696
$Eu:LaF_3$	Tm:gls	$^7F_6$	$^7F_6$	$^7F_4$	3.9–5.4	696	627
$Eu:LaF_3$	Tm:gls	$^7F_6$	$^7F_6$	$^7F_3$	3.0–3.4	627	734
$Tb:LaF_3$	Ho:YAG	$^7F_3$	$^7F_3$	$^7F_4$	8.0–15.0	646	954
$Tb:LaF_3$	Ho:YAG	$^7F_3$	$^7F_3$	$^7F_5$	4.1–5.0	954	1772
$Dy:LaF_3$	Nd:YAG	$^6F_{9/2}$	$^6H_{9/2}$	$^6H_{11/2}$	5.4–6.2	1605	2196
$Dy:LaF_3$	Er:YLF	$^6H_{11/2}$	$^6H_{11/2}$	$^6H_{13/2}$	4.0–4.5	2196	3178
$Ho:LaF_3$	Tm:gls	$^5I_5$	$^4I_5$	$^5I_6$	3.7–4.0	2467	3416
$Ho:LaF_3$	Nd:YAG	$^5I_6$	$^5I_6$	$^5I_7$	2.9–3.4	3416	4782
$Er:LaF_3$	Cr:alex	$^4I_{9/2}$	$^4I_{9/2}$	$^4I_{11/2}$	4.1–4.9	2024	3478
$Er:LaF_3$	Er:YAG	$^4I_{9/2}$	$^4I_{11/2}$	$^4I_{13/2}$	2.6–2.9	3478	6161
$Tm:LaF_3$	diode	$^3H_5$	$^3H_5$	$^3F_4$	3.6–4.5	2290	5227

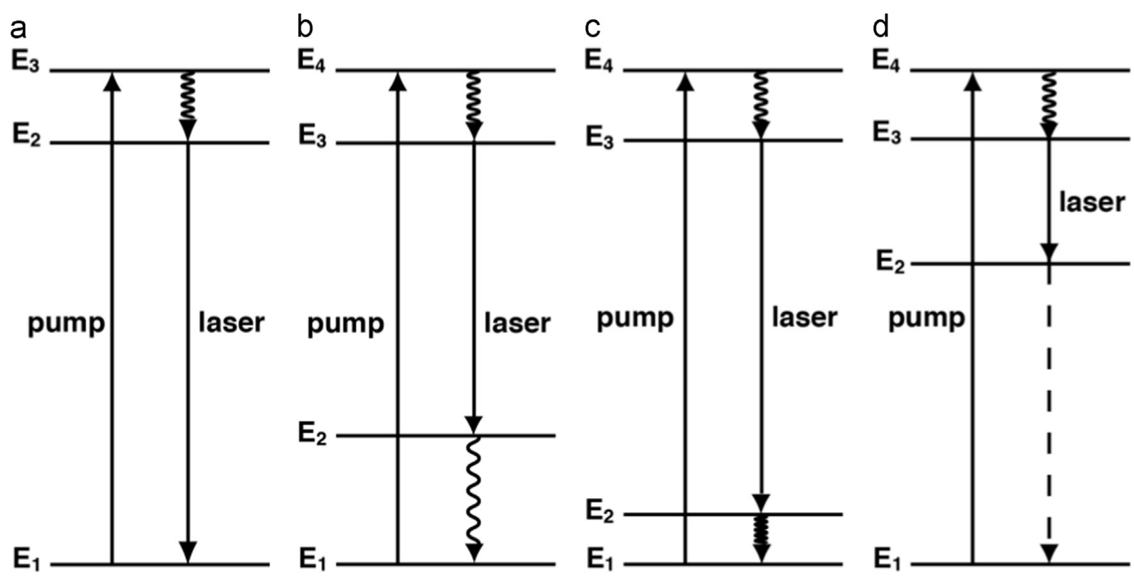

Fig. 4. Types of solid state lasers: (a) 3-level; (b) 4-level; (c) quasi 4-level; and (d) terminated 4-level.

2.1.4. Europium

A Eu laser can be pumped from the $^7F_0$ manifold to the $^7F_6$ manifold with a Tm:fiber or diode laser. From the $^7F_6$ manifold, there are several possible choices for generating mid infrared radiation in both 3–5 μm and the 7–12 μm regions. Because the $^7F_6$ and $^7F_5$ manifolds have a small separation, the laser material must have a very low phonon energy for the $^7F_6$ manifold to be an efficient storage manifold. There are several possibilities for cascade lasers. Infrared laser action of Eu depends on Q-switched laser action from the $^7F_6$ manifold. When this manifold is Q-switched, population inversions can be established between the $^7F_6$ manifold and both the $^7F_4$ and the $^7F_3$ manifolds in spite of the small energy gaps to the next laser manifold. These transitions produce an output in the 3–5 μm. Both lower laser manifolds are sufficiently above the ground level so that the thermal population of the lower laser level is small.

2.1.5. Terbium

Tb lasers can be pumped into the $^7F_3$ manifold with a Tm or a Ho laser. Either a fiber laser or a bulk laser can be used for pumping. If a high energy per pulse is needed, the energy may have to be stored in the pump laser. Lifetime depends on energy gap to next lower manifold and material properties. If nonradiative quenching is the major decay mechanism, the smaller gap indicates a shorter lifetime. However, if monradiative quenching is a minor decay mechanism, energy storage can take advantage of the full radiative lifetime, assuming no influences from energy transfer processes. Unfortunately, pumping into the $^7F_4$ manifold is less practical because the wavelength of the pump laser would already be in the mid infrared. From the $^7F_3$ manifold both the 4–5 μm transitions, $^7F_3$ manifold to the $^7F_5$, manifold and the 8–15 μm transitions, $^7F_3$ manifold to the $^7F_{4,}$ manifold, appear possible.

2.1.6. Dysprosium

A Dy laser can be pumped by an Er:YLF laser or a Tm:YLF laser. Pumping would use the $^6H_{15/2}$ manifold to the $^6H_{11/2}$ manifold transition. Laser action can occur between the $^6H_{11/2}$ manifold and the $^6H_{13/2}$ manifolds, providing an output in the 3.0–5.0 μm region. Because the energy gap between the $^6H_{13/2}$ manifold and the $^6H_{15/2}$ manifold is so large, it is expected that this will be a terminated

4 level laser. However, codoping with a second Lanthanide series atom can provide an alternate path to the ground manifold and mitigate this effect. Laser action on this transition at 4.34 μm using an Er:YLF laser operating at 1.73 μm has already been demonstrated [4].

2.1.7. Holmium

A Ho laser can be pumped with 1.9 μm diodes, which are available. The $^5I_5$ manifold could be pumped by a frequency doubled Tm: fiber laser. The Ho $^5I_8$ to $^5I_6$ transition could be pumped by using some of the less common transition of the Nd:YAG laser. The energy gap between the $^5I_5$ and the next lower laser level is large enough so that the $^5I_5$ manifold could store energy efficiently in a low phonon energy material. Laser action would occur between the $^5I_5$ and the $^5I_6$ manifold around 3.7–4.0 μm. The energy gap between the $^5I_6$ manifold and the $^5I_7$ manifold is large indicating the possibility that this is a terminated 4 level laser. Co-doping with another lanthanide series atom, such as Sm or Tm, to relax the lower laser manifold can mitigate the effects associated with a terminated 4 level laser. A better solution would be cascade lasing between the $^5I_6$ and the $^5I_7$ manifolds. This would produce an output in the 2.9–3.4 μm range.

2.1.8. Erbium

Er lasers can be directly pumped utilizing diode lasers. To take further advantage of this, the laser may have to be co-doped with Yb. The Yb will absorb high power GaAs pump radiation and then transfer the energy to the Er $^4I_{11/2}$ manifold. In addition, it is possible to pump an Er laser with a pump that operates at about 1.5 μm. At high densities of Er in the $^4I_{13/2}$ manifold, up conversion can occur where 2 nearby Er atoms in the $^4I_{13/2}$ manifold interact to promote an Er atom to the $^4I_{9/2}$ manifold and to demote the other Er atom to the $^4I_{15/2}$ manifold. From there the excited Er atom relaxes to the $^4I_{11/2}$ manifold. This increases the population inversion by 3, with 2 less Er atoms in the lower laser manifold, $^4I_{13/2}$, and 1 more atom in the lower laser manifold, $^4I_{11/2}$. Laser action could occur between the Er $^4I_{11/2}$ manifold and $^4I_{13/2}$ manifold [5]. Finally, it is possible to pump the Er laser with a Cr: alexandrite, laser for producing a laser on the $^4I_{9/2}$–$^4I_{11/2}$ in the 4–5 μm region. This pump laser has the distinct advantage of wavelength tuning. This allows the pump laser to be tuned to a strong absorption feature.

2.1.9. Thulium

A Tm laser has no obvious pump lasers, but diode lasers pumping the $^3H_5$ manifold may be used if available. The transition from $^3H_5$ to $^3F_4$ produces wavelengths in the 3–5 μm region, but is likely a terminated 4-level laser.

3. Experimental

The energy levels of lanthanide series atoms determine the laser wavelength. To first order, pairs of energy levels that can generate the mid infrared laser wavelengths are determined by the 4f electron energy levels of the lanthanide series atom. To minimize non-radiative quenching of the mid infrared transition, there should be no intervening energy levels between the upper and the lower laser manifolds. Although the energy levels may be known, this does not guarantee that a particular pair of energy levels will be useful. To determine if a pair of energy levels is useful, a sufficiently large transition probability between the participating energy levels must exist. NASA Langley has a quantum mechanical model that calculates level-to-level transition probabilities for such assessments, but it is outside the scope of this article.

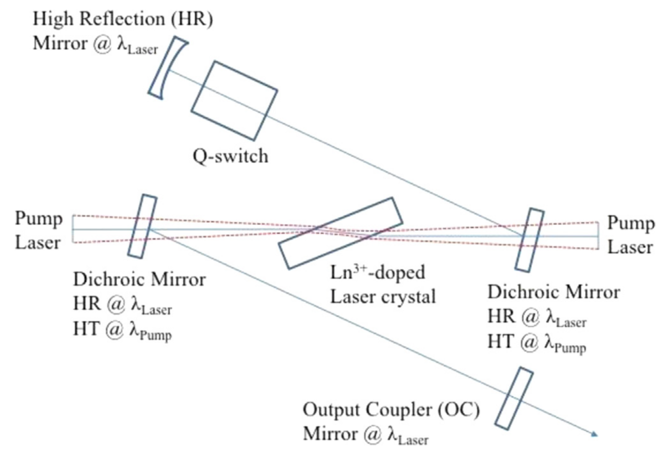

Fig. 5. End pumped Z-type resonator design.

3.1. Laser design

An end pumped laser design provides several advantages for mid infrared lasers. Mid infrared lasers are often terminated 4-level or quasi 4-level lasers, the later sometimes exhibiting low gain. The end-pumping configuration combats the negative impact of these conditions in an efficient manner. The gain is concentrated along the axis of the laser beam with no apertures to limit extraction efficiency. A tentative laser design helps define what laser properties are important for optimization in the search for and demonstration of mid infrared lasers.

An efficient end pumped design is proposed for the mid infrared lasers, shown in Fig. 5. The pump can be a fiber coupled diode laser, a fiber laser, or a bulk solid state laser. Diode pumped solid-state lasers have become the de facto laser of choice for a myriad of applications. The reasons for this are the combination of high reliability, long life, good efficiency, and the ability to store energy and extract it in a single short pulse, i.e., a Q-switched pulse. Fig. 5 depicts a fiber coupled diode laser. However, a diode pumped fiber laser would be similar. In this configuration the laser rod can be pumped from both ends which doubles the total pump power. In other configurations, the pump beam can be double passed which promotes efficient absorption. In addition, if the pump is polarized, a polarization dependent beam combiner can combine 2 pump beams. This almost doubles the available pump power again. Therefore, high gains are possible even when the emission cross section is relatively small. End pumping also allows an optimum overlap of the pumped volume and the mode volume of the mid infrared laser. Designing the pumped volume to be small compared with the cross section of the laser medium, deleterious diffraction effects are avoided. Also, the pump laser can serve as the energy storage device. If there are no suitable long lifetime, mid infrared manifolds in which to store the energy, energy can stored in the pump laser. The stored energy can then be transferred to the mid infrared laser quickly by Q-switching the pump laser.

3.2. Pr-doped laser material spectroscopy

A natural first step in assessing the laser potential of any of the laser transitions discussed in this article is the measurement of its emission spectrum. Here we demonstrate emission of $Pr:LaF_3$ and $Pr:KPb_2Br_5$ in the 3–6 μm region. As illustrated in Fig. 6, the cross sections are of a reasonable size for laser operation. A more extensive presentation of Pr MIR emission in a variety of hosts will be published elsewhere.

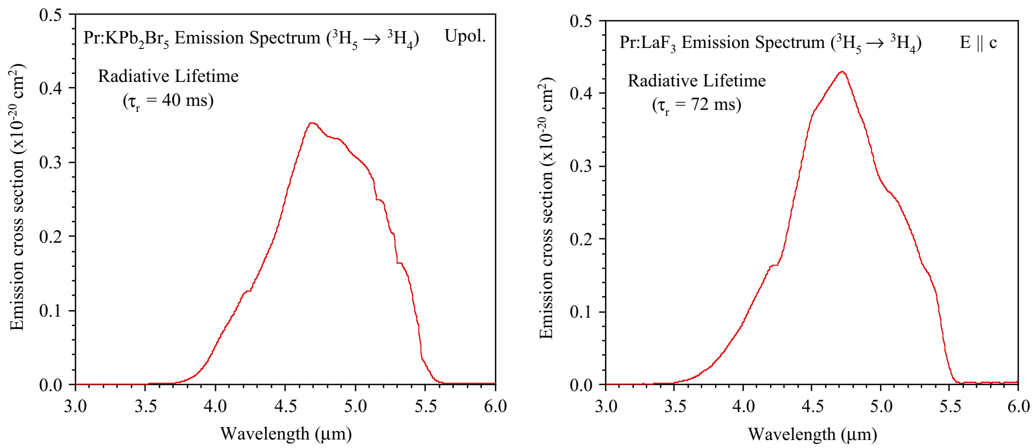

Fig. 6. Emission of Pr:KPb_2Br_5 (left) and Pr:LaF_3 (right) from 3 to 6 μm. U-pol. Indicates that the spectra is unpolarized. *E*||*c* indicates p-polarization.

4. Conclusions

Potential laser materials are selected primarily on the basis of its phonon spectra. In the future, other laser material properties will become important, such as thermal conductivity. However, these effects depend on the particular laser design. In turn, this depends on the particular application. As a consequence, it is premature to consider the other parameters at this time. Preliminary resonator design has been considered.

LaF_3 is a good choice for the laser material. The maximum phonon energy, 300–350 cm^{-1}, is acceptable in the lower range of values acceptable. It has a natural 3+ site with the right size for doping with a lanthanide series atom. Some materials do not have a natural 3+ site. If the lanthanide series atom substitutes in a 2+ site for example, charge compensation is required which complicates growth and tends to increase the line width. KPb_2Br_5 is also a good choice for a laser material. The maximum phonon energy is around 140 cm^{-1} [6]. In potassium lead halides the Ln^{3+} ions substitute for Pb^{2+} ions at different sites forming a vacancy with charge compensation [7]. Measurement of emission for Pr in these hosts in the 3–6 μm region has been demonstrated to illustrate the viability of these materials for MIR lasers.

Acknowledgment

The authors would like to thank A. Yoshikawa at Tohoko University in Sendai, Japan for growing the Pr:LaF_3 sample and U. Hommerich of Hampton University, Hampton, VA, USA for providing the Pr:KPb_2Br_5 sample.

References

[1] Anon, Earth Science and Applications from Space-National Imperatives for The Next Decade and Beyond, The National Academics Press, Washington, DC, 2007.
[2] F.K. Tittel, D. Richter, A. Fried, Mid-infrared laser applications in spectroscopy, Springer-Verlag (2003) 445, Solid-State Mid-Infrared Laser Sources.
[3] S.R. Bowman, L.B. Shaw, B.J. Feldman, J. Ganem, IEEE J. Quantum Electron. 32 (1996) 646.
[4] N.P. Barnes, R.E. Allen, IEEE J. Quantum Electron. (1991) 277, QE-27.
[5] S.A. Pollack, D.B. Chang, J. Appl. Phys. 64 (1988) 2885.
[6] L. Isaenko, Mid Infrared Coherent Sources and Applications, Springer, Dordrecht, The Netherlands (2008) 3–59.
[7] A.M. Tkachuk, S.E. Ivanova, L.I. Isaenko, A.P. Yelisseyev, S. Payne, R. Solarz, R. Page, M. Norstrand, Opt. Spectrosc. 92 (2002) 83.